Lattice study of the massive Schwinger model with a θ term under Lüscher's "admissibility" condition

Hidenori Fukaya and Tetsuya Onogi
Yukawa Institute for Theoretical Physics, Kyoto University, Kyoto 606-8502, Japan
(Received 31 May 2003; published 23 October 2003)

Lüscher's "admissibility" condition on the gauge field space plays an essential role in constructing lattice gauge theories which have exact chiral symmetries. We apply the gauge action proposed by Lüscher with the domain-wall fermion action to the numerical simulation of the massive Schwinger model. We find this action can generate configurations in each topological sector separately without any topology changes. By developing a new method to sum over different topological sectors, we calculate the meson masses in the nonzero θ vacuum.

DOI: 10.1103/PhysRevD.68.074503 PACS number(s): 12.38.Gc

I. INTRODUCTION

There are various problems in gauge theories in which chiral symmetry plays a crucial role. Although lattice gauge theories provide a method for nonperturbative computation on these problems, they have not given satisfactory answers since the conventional fermion action suffers from either species doubling [1–3] or a lack of chiral symmetry, which makes the study of chiral behavior difficult. For this reason, extensive studies have been made to improve the fermion action. It was found that lattice Dirac operators satisfying the Ginsparg-Wilson relation [4], which is, for example, realized by the Neuberger's overlap Dirac operator [5,6], have exact chiral symmetries [7]. Such actions are expected to give a fundamental improvement in the study of K meson physics, finite temperature QCD, or even chiral gauge theories, despite their complicated forms.

At the classical level, the Ginsparg-Wilson relation is sufficient to solve the problem of chirality. However, at the quantum level, the topological properties of the gauge fields in the continuum space should also be kept on the lattice in order to reproduce the correct chiral anomalies. Lüscher found that one can construct lattice gauge theories without breaking topological structures by restricting the link variables to satisfy the "admissibility condition" [8]

$$\|1-P_{\mu\nu}(x)\|<\epsilon \quad \text{for all} \quad x,\mu,\nu, \tag{1}$$

where

$$P_{\mu\nu}(x)=U_\mu(x)U_\nu(x+\hat{\mu}a)U_\mu^\dagger(x+\hat{\nu}a)U_\nu^\dagger(x), \tag{2}$$

and ϵ is a fixed positive number. In order for the gauge fields to satisfy this condition automatically, he proposed the following action as an example:

$$S_G=\begin{cases}\beta\displaystyle\sum_{x,\mu>\nu}\frac{[1-\mathrm{Re}\,P_{\mu\nu}(x)]}{1-\|1-P_{\mu\nu}(x)\|/\epsilon} & \text{if } \|1-P_{\mu\nu}(x)\|<\epsilon,\\ \infty & \text{otherwise.}\end{cases} \tag{3}$$

The admissibility condition makes gauge fields smooth and unphysical configurations such as vortices are suppressed. In fact, the space of admissible fields is separated into disconnected subspaces labeled by integers which correspond to topological charges in the continuum theory [9,10]. Therefore one can precisely treat topological effects such as the U(1) problem, θ vacuum, and so on. Moreover, Lüscher's action is also differentiable and gauge invariant and has a good continuum limit as does Wilson's action.

Although there are other proposals for improvements of the gauge action [11–17], they do not keep any topological structures. In this sense Lüscher's action combined with Ginsparg-Wilson fermion action would be the best choice to investigate chiral symmetries on the lattice. Moreover, an admissibility condition is indispensable to construct chiral gauge theories since the gauge symmetry is never realized without exact chiral symmetries [8,18]. Thus it would be important to examine how admissibility works and how topological structures are realized on the lattice in numerical simulations.

In this paper, we apply Lüscher's gauge action to the numerical studies of the two-flavor massive Schwinger model [19] on the lattice using the domain wall fermion action [20,21] in order to examine how the admissibility works by probing the topological properties of the lattice theories. The massive Schwinger model is a good test ground for several reasons; it has been well examined analytically in continuum space even in strong coupling limit, its vacuum has nontrivial topological structures due to the chiral anomaly, and it also shares many other interesting properties with QCD such as the U(1) problem and the confinement. There already exist extensive studies of topological structures of the massive Schwinger model on the lattice with Wilson's gauge action in the literature [22–28], where our work provides an alternative lattice approach with Lüscher's action. Although it will be an interesting subject to make a detailed comparison of the results with our method with previous calculations, we will leave it for future publications and focus on the feasibility study of our method and new results on θ vacuum in the present work.

We found that Lüscher's gauge action can generate configurations in each topological sector separately. We develop a new method to evaluate the observables in nonzero-θ vacuum by summing over those in different sectors with cor-

rect weights. (Our strategy is quite different from that of sampling other sectors by enhancing topology changes [29–32].) We applied our method to the meson correlators and observe the θ dependence of the isotriplet meson mass. We reproduce well-known continuum results; the isotriplet meson mass scaling as a function of the fermion mass and their θ dependence, and the fact that the isosinglet meson acquires a heavier mass than the isotriplet meson due to anomaly [the so-called U(1) problem].

This paper is organized as follows. In Sec. II, we summarize the main results of the continuum massive Schwinger model. In Sec. III, we discuss details of our simulation. In Sec. IV, we present the results and compare them with continuum theory. In the Appendix, we compare Lüscher's action and Wilson's action in the quenched approximation, and show the impact of the admissibility condition on the topological and chiral properties.

II. REVIEW OF THE MASSIVE SCHWINGER MODEL

A. Continuum theory

We consider the two flavor massive Schwinger model [33–35] with degenerate masses. The continuum action in Euclidean space is defined as

$$S = S_G + S_F,$$

$$S_G = \int d^2x \frac{1}{4g^2} F_{\mu\nu}(x) F^{\mu\nu}(x),$$

$$S_F = \int d^2x \sum_{i=1}^{2} \bar{\psi}_i(x)(\not{D} + m)\psi_i(x), \tag{4}$$

where

$$F_{\mu\nu}(x) = \partial_\mu A_\nu(x) - \partial_\nu A_\mu(x), \quad \not{D} = \sum_{\mu=1}^{2} \gamma^\mu(\partial_\mu + iA_\mu),$$

$$\gamma^1 = \begin{pmatrix} 0 & 1 \\ 1 & 0 \end{pmatrix}, \quad \gamma^2 = \begin{pmatrix} 0 & -i \\ i & 0 \end{pmatrix}, \quad \gamma^3 = -i\gamma^1\gamma^2, \tag{5}$$

A_μ is the gauge field and ψ is the two-spinor fermion field. We take g and m to be positive without losing generality.

If we take the space-time to be a torus T^2, the space of gauge fields is separated into topological sectors each of which is labeled by an integer

$$N = \frac{1}{4\pi} \int_{T^2} d^2x \epsilon_{\mu\nu} F^{\mu\nu}, \tag{6}$$

where we take the sign convention of the antisymmetric tensor as $\epsilon_{12} = 1$. Then this theory has vacua dependent on phase θ. The full path integral is defined by a summation of integrals in each topological sector;

$$Z_{\text{full}}(g,m,\theta) = \sum_{N=-\infty}^{+\infty} e^{iN\theta} Z_N(g,m),$$

$$Z_N(g,m) = \int DA_\mu^N D\bar{\psi} D\psi \exp(-S_G - S_F), \tag{7}$$

where A_μ^N denotes the gauge fields in the sector with topological charge N. Using Eq. (6), we can rewrite $Z_{\text{full}}(g,m,\theta)$ as follows:

$$Z_{\text{full}}(g,m,\theta) = \int DA_\mu D\bar{\psi} D\psi \exp(-S_G - S_F - S_\theta), \tag{8}$$

where

$$S_\theta = -i \int d^2x \frac{\theta}{4\pi} \epsilon_{\mu\nu} F^{\mu\nu}. \tag{9}$$

It is well-known that this model is equivalent to the two-component scalar theory [34–36]

$$S = \int d^2x \left[\frac{1}{2} \partial_\mu \phi_+(x) \partial^\mu \phi_+(x) + \frac{1}{2} \partial_\mu \phi_-(x) \partial^\mu \phi_-(x) + \frac{\mu_0^2}{2} [\phi_+(x)]^2 - 2cmg \times \cos\left(\sqrt{2\pi}\phi_+(x) - \frac{\theta}{2} \right) \cos[\sqrt{2\pi}\phi_-(x)] \right], \tag{10}$$

where $\mu_0 = g\sqrt{2/\pi}$ and c is a numerical constant.

For $m \ll \mu_0$ and $\theta \sim 0$, perturbative calculations of $O(m)$ show that light scalar ϕ_- has the mass

$$m_- = \sqrt{2\pi} \left(2cm\mu_0^{1/2} \cos\frac{\theta}{2} \right)^{2/3}, \tag{11}$$

and heavy scalar ϕ_+ has the mass

$$m_+ = \mu_0 + [O(m) \text{ corrections}]. \tag{12}$$

Now, we discuss the chiral behaviors of the two-flavor Schwinger model in the chiral limit $m \to 0$. The action has $U(2)_A \simeq SU(2)_A \times U(1)_A$ chiral symmetry in this limit. $U(1)_A$ symmetry is broken by the anomaly, which manifests itself in the vacuum with nontrivial topological structures. We define the isotriplet meson operator $\pi_0 \equiv \bar{\psi}_1 \gamma_3 \psi_1 - \bar{\psi}_2 \gamma_3 \psi_2$ and the isosinglet meson operator $\eta \equiv \bar{\psi}_1 \gamma_3 \psi_1 + \bar{\psi}_2 \gamma_3 \psi_2$ by the fermion bilinears. In the bosonization picture, it is shown that π_0 propagation corresponds to that of light scalar ϕ_- and η propagation corresponds to that of heavy scalar ϕ_+. In the massless limit, Eqs. (11) and (12) show that π_0 becomes massless while η remains massive in accordance with the U(1) problem in two-dimensional QED.

B. Lattice theory

Let us consider the lattice regularization of the massive Schwinger model. We take the lattice size as $L \times L \times L_3$ with

lattice spacing $a=1$, where L_3 is the length of the third direction for the domain wall fermions [20,21]. The action is defined as follows:

$$S=\beta S_G+S_F, \tag{13}$$

$$S_G=\begin{cases}\displaystyle\sum_P \frac{[1-\mathrm{Re}\,P_{\mu\nu}(x)]}{1-[1-\mathrm{Re}\,P_{\mu\nu}(x)]/\epsilon} & \text{if admissible,}\\ \infty & \text{otherwise,}\end{cases} \tag{14}$$

$$S_F=\sum_{x,x'}\sum_{s,s'}\sum_{i=1}^{2}[\overline{\psi}^i_s(x)D_{DW}(x,s;x',s')\psi^i_{s'}(x') + \phi^{i*}_s(x)D_{AP}(x,s;x',s')\phi^i_{s'}(x')], \tag{15}$$

where

$$\begin{aligned}D_{DW}(x,s;x',s') &= \frac{1}{2}\sum_{\mu=1}^{2}\{(1+\gamma_\mu)U_\mu(x)\delta_{x+\hat{\mu},x'}\delta_{s,s'}\\ &+(1-\gamma_\mu)U^\dagger_\mu(x-\hat{\mu})\delta_{x-\hat{\mu},x'}\delta_{s,s'}\}\\ &+(M-3)\delta_{x,x'}\delta_{s,s'}+P_+\delta_{s+1,s'}\delta_{x,x'}\\ &+P_-\delta_{s-1,s'}\delta_{x,x'}+(m-1)P_+\delta_{s,L_3}\delta_{s',1}\delta_{x,x'}\\ &+(m-1)P_-\delta_{s,1}\delta_{s',L_3}\delta_{x,x'},\end{aligned}$$

$$\begin{aligned}D_{AP}(x,s;x',s') &= \frac{1}{2}\sum_{\mu=1}^{2}\{(1+\gamma_\mu)U_\mu(x)\delta_{x+\hat{\mu},x'}\delta_{s,s'}\\ &+(1-\gamma_\mu)U^\dagger_\mu(x-\hat{\mu})\delta_{x-\hat{\mu},x'}\delta_{s,s'}\}\\ &+(M-3)\delta_{x,x'}\delta_{s,s'}+P_+\delta_{s+1,s'}\delta_{x,x'}\\ &+P_-\delta_{s-1,s'}\delta_{x,x'}-2P_+\delta_{s,L_3}\delta_{s',1}\delta_{x,x'}\\ &-2P_-\delta_{s,1}\delta_{s',L_3}\delta_{x,x'}.\end{aligned} \tag{16}$$

$\beta=1/g^2$, M is a constant satisfying $0<M<1$, Σ_P denotes summation over all plaquettes, and $P_\pm$ are the chiral projection operators;

$$P_\pm=\frac{1\pm\gamma_3}{2}. \tag{17}$$

m is the fermion mass. ϕ^i's are Pauli-Villars regulators which cancel the bulk contribution.

Since it is not possible to change the topological charge by a local updating under the admissibility condition, our lattice theory with Lüscher's gauge action has a topological invariant,

$$N=-\frac{i}{2\pi}\sum_x \ln P_{12}(x). \tag{18}$$

This charge corresponds to Eq. (6) and gauge field configurations are classified into topological sectors. Each sector characterized by N has the classical gauge configuration $U^{cl}_\mu(x,y)$ minimizing the action, which is given in Eq. (7.10) of Ref. [8] as

$$\begin{aligned}U_1^{cl[N]}(x,y)&=\exp\left\{\frac{2\pi i\nu_1}{L}-\frac{2\pi Ni}{L}\delta_{x,L}y\right\},\\ U_2^{cl[N]}(x,y)&=\exp\left\{\frac{2\pi i\nu_2}{L}+\frac{2\pi Ni}{L^2}x\right\},\end{aligned} \tag{19}$$

up to gauge transformations, where ν_1 and ν_2 are the parameters which determine the values of Wilson lines in x and y directions. $\nu_{1,2}$ can take any values in the region $0\leqslant\nu_{1,2}<1$. This configuration gives constant background electric fields over the torus.

III. LATTICE SIMULATIONS

A. Observables in each sector

The simulation is carried out by the hybrid Monte Carlo method with Lüscher's gauge action in Eq. (14). The matrix inversions are calculated by the conjugate gradient algorithm.

We take a $16\times16\times6$ lattice at $\beta=1/g^2=0.5$ and $M=0.9$. The parameter for the admissibility condition is chosen as $\epsilon=1.0$. At this value of ϵ, we find that initial topological charge is not changed through the simulation. (See Fig. 1.) For the fermion mass, we choose $m=0.1,0.2,0.3,0.4$. Fifty molecular dynamics steps with a step size $\Delta\tau=0.02$ are performed in one trajectory of the hybrid Monte Carlo algorithm. Configurations are updated per ten trajectories. We generate 500 configurations for each topological sector by taking the classical configuration in Eq. (19) as the initial configuration. From the set of configurations in each sector with topological charge N, we measure the isotriplet meson propagator

$$C_\pi(x)=\sum_y\langle\pi(x,y)\pi(0,0)\rangle^N_{\beta,m}, \tag{20}$$

and the isosinglet meson propagator

$$C_\eta(x)=\sum_y\langle\eta(x,y)\eta(0,0)\rangle^N_{\beta,m}, \tag{21}$$

where $\langle\ \rangle^N_{\beta,m}$ denotes the expectation value in the N sector.

B. A new method of summing over different topological sectors

The hybrid Monte Carlo simulation is performed by small changes of link variables. Thus choosing the configuration given by Eq. (19) as the initial condition, we can generate configurations without changing the topological charge for any value of the coupling constant.

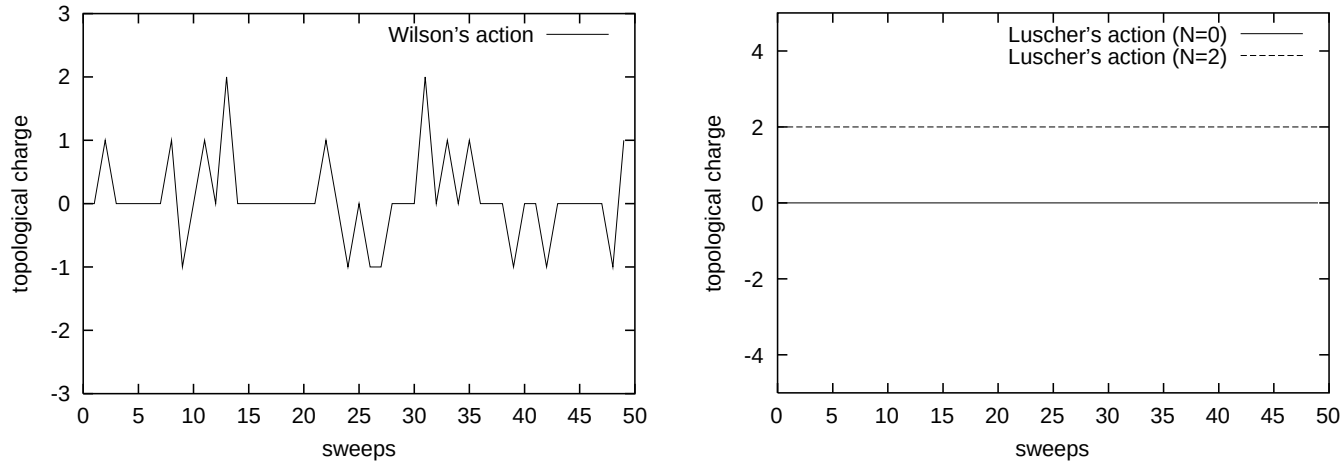

FIG. 1. The comparison of the Monte Carlo evolution of the topological charge with Wilson's gauge action and Lüscher's gauge action. $\beta=2.0$ with Lüscher's gauge action and $\beta=0.5$ with Wilson's gauge action correspond to roughly the same lattice spacing from the string tension which is obtained from the logarithm of the plaquette expectation value in the $N=0$ sector. Left: Wilson's gauge action with $\beta=2.0$. Initial topological charge is zero. Right: Lüscher's gauge action with $\beta=0.5$. The solid line shows the case when the initial charge is zero and the dashed line shows the case when the initial topological charge is two. The topological charge changes for Wilson's gauge action, while it does not for Lüscher's action.

Now, we discuss full path integrals on the θ vacuum. Suppose that we measure the expectation value of an operator O,

$$\langle O\rangle^{\rm full}_{\beta,m}=\frac{\sum_{N=-\infty}^{+\infty} e^{iN\theta}\int DU^N_\mu D\bar{\psi}D\psi O e^{-\beta S_G-S_F}}{\sum_{N=-\infty}^{+\infty} e^{iN\theta}Z_N(\beta,m)}, \quad (22)$$

where U^N_μ denotes link variables in the sector with N and

$$Z_N(\beta,m)=\int DU^N_\mu D\bar{\psi}D\psi e^{-\beta S_G-S_F} \quad (23)$$

is the lattice counterpart of the Z_N in Eq. (7). In terms of the expectation values in each topological sector, $\langle O\rangle^{\rm full}_{\beta,m}$ can be rewritten as

$$\langle O\rangle^{\rm full}_{\beta,m}=\frac{\sum_{N=-\infty}^{+\infty} e^{iN\theta}\langle O\rangle^N_{\beta,m}R^N(\beta,m)}{\sum_{N=-\infty}^{+\infty} e^{iN\theta}R^N(\beta,m)}, \quad (24)$$

where

$$\langle O\rangle^N_{\beta,m}=\frac{\int DU^N_\mu D\bar{\psi}D\psi O e^{-\beta S_G-S_F}}{Z_N(\beta,m)}, \quad (25)$$

and

$$R^N(\beta,m)=\frac{Z_N(\beta,m)}{Z_0(\beta,m)}. \quad (26)$$

We call $R^N(\beta,m)$ the reweighting factor. Note that $Z_N(\beta,m)$ satisfies the following differential equation:

$$\frac{\partial Z_N(\beta,m)}{\partial\beta}\Big/ Z_N(\beta,m)=-\langle S_G\rangle^N_{\beta,m}. \quad (27)$$

By integrating over β again, $Z_N(\beta,m)$ is expressed as

$$Z_N(\beta,m)=Z_N(\infty,m)\exp\left(\int_\beta^\infty d\beta'\langle S_G\rangle^N_{\beta',m}\right). \quad (28)$$

Then, the reweighting factor $R^N(\beta,m)$ is expressed as

$$\begin{aligned}R^N(\beta,m)&=\frac{Z_N(\infty,m)}{Z_0(\infty,m)}\exp\left[\int_\beta^\infty d\beta'(\langle S_G\rangle^N_{\beta',m}-\langle S_G\rangle^0_{\beta',m})\right]\\&=\exp(-\beta S^N_{G\,\rm min})\frac{\int d\nu_1 d\nu_2\,\det(D^N_{DW})^2/\det(D^N_{AP})^2}{\int d\nu_1 d\nu_2\,\det(D^0_{DW})^2/\det(D^0_{AP})^2}\\&\quad\times\exp\left[\int_\beta^\infty d\beta'(\langle S_G-S^N_{G\,\rm min}\rangle^N_{\beta',m}-\langle S_G\rangle^0_{\beta',m})\right],\end{aligned} \quad (29)$$

where $S^N_{G\,\rm min}$ is the minimum of the gauge action in the sector with N given by constant background fields Eq. (19) and D^N_{DW} and D^N_{AP} are Dirac operators given by this background. Note that the integrand vanishes rapidly as $\beta'\to\infty$, so the integral over β' converges.

We can evaluate the full path integrals on the θ vacuum by obtaining $\langle O\rangle^N_{\beta,m}$ and $R^N(\beta,m)$ in each sector. It should be noted that this method is only possible with a gauge action with the admissibility condition in which the topological charge is strictly conserved. In our approach we take the

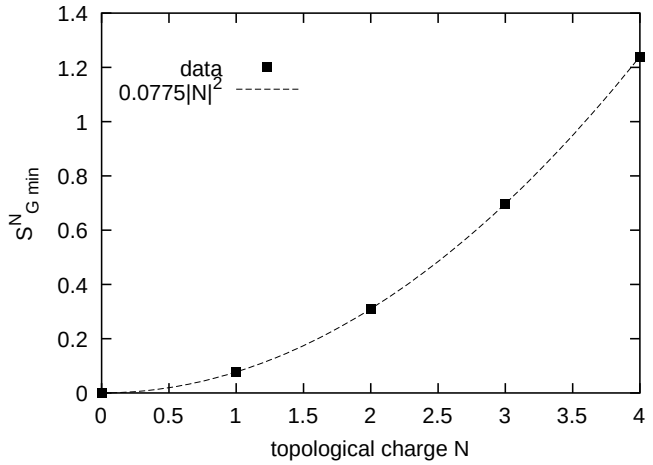

FIG. 2. Minimum action in each topological sector is plotted as a function of the topological charge. Closed squares are the data and the dashed line is the fit with a quadratic function.

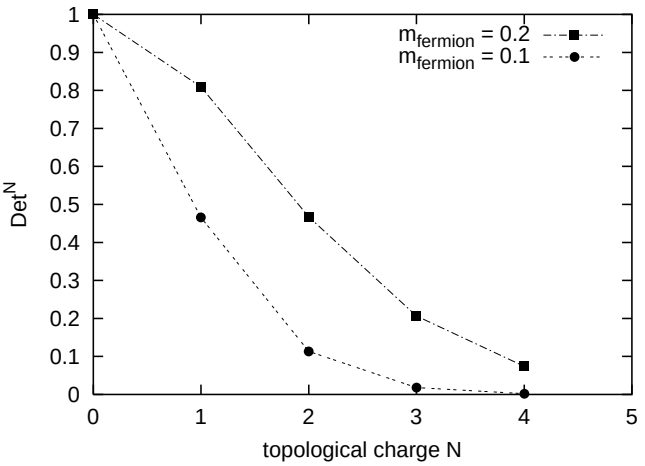

FIG. 4. $|N|$ dependence of Det^N for the fermion mass $m=0.1,0.2$ is shown.

property that Lüscher's gauge action allows no topology change at all as an advantage and treat the sum over the topologies in a controlled fashion. This is in contrast to the conventional gauge actions, with which the topology change is suppressed but not completely prohibited so that one has to tackle the problem of enhancing topology changes.

A related but somewhat different approach was proposed by Dürr [37] where one makes a quenched calculation and give the whole fermion determinant as the reweighting factor. He also proposed an approximation in which one replaces the determinant for the given configuration by the determinant of a common representative configuration for the given sector, which reduces the enormous computational effort.

Of course, computing the reweighting factors for the sum over topologies requires extra work. Whether this program works must be examined in practical simulations. In the following sections we show that our new method is valid and full path integrals can be evaluated with controlled statistical and systematic errors.

C. Calculation of $R^N(\beta,m)$

Let us discuss how to evaluate $R^N(\beta,m)$. The classical minima of the gauge action $S^N_{G\ \mathrm{min}}$ are evaluated easily. In Fig. 2, we can see that $S^N_{G\ \mathrm{min}}$ is numerically proportional to $|N|^2$.

The fermion determinant $\det D^2$ on classical background in the sector with N is numerically calculated using the Householder method and the QL method [38]. The integral over the moduli $\nu_{1,2}$ is approximated by the weighted sum over the discrete set of points uniformly distributed in the whole integration region as in Fig. 3. The number of points for the weighted sums are 5×5 for both $\det(D^0_{DW})^2/\det(D^0_{AP})^2$ and for $\det(D^N_{DW})^2/\det(D^N_{AP})^2$ with $N\neq0$. The value of

$$\mathrm{Det}^N \equiv \frac{\int d\nu_1 d\nu_2\, \det(D^N_{DW})^2/\det(D^N_{AP})^2}{\int d\nu_1 d\nu_2\, \det(D^0_{DW})^2/\det(D^0_{AP})^2} \tag{30}$$

is plotted in Fig. 4. It decreases as $|N|$ increases, due to the contribution of small eigenvalues proportional to the fermion

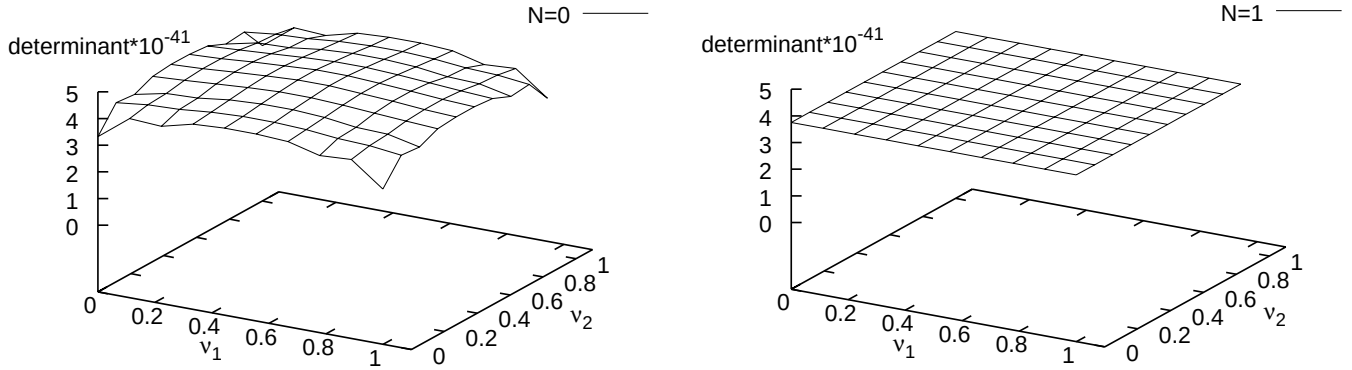

FIG. 3. Three-dimensional plot of the ν dependence of the fermion determinant $\det(D^N_{DW})^2/\det(D^N_{AP})^2$. Left: $N=0$ case, right: $N=1$ case.

TABLE I. The value of $\int d\beta' S^N_{\rm subtr}$ in each sector.

Topological charge	$\int d\beta' S^N_{\rm subtr}$	Error
0	0	0
1	−0.201	0.088
2	0.099	0.088
3	0.32	0.12
4	0.47	0.14

mass, which emerge in the nontrivial topological sectors since the Atiyah-Singer index theorem is realized on the lattice in the $L_3\to\infty$ limit [7].

In order to obtain the exponential factor in Eq. (29), we need to evaluate the integral of the following quantity

$$S^N_{\rm subtr}(\beta',m)\equiv\langle S_G - S^N_{G\ \rm min}\rangle^N_{\beta',m} - \langle S_G\rangle^0_{\beta',m}. \qquad (31)$$

Since $S^N_{\rm subtr}(\beta',m)$ decreases rapidly as $\beta'\to\infty$, the integral of $S^N_{\rm subtr}$ over β' is well approximated by a weighted sum over the discrete set of points for $S^N_{\rm subtr}(\beta',m)$ at $\beta'=0.5,1.0,1.5,2.0$. For each β', we evaluate $S^N_{\rm subtr}(\beta',m)$ by sampling more than 5000 configurations. The results are summarized in Table I.

Total reweighting factor $R^N(\beta,m)$ at $\beta=0.5$ and $m=0.2$ is plotted in Fig. 5. It is shown that higher topological sectors are indeed suppressed by the reweighting factor.

Finally, combining the correlators and the reweighting factors, we obtain the total expectation values on the nonzero-θ vacuum as

$$\sum_y \langle \pi(x,y)\pi(0,0)\rangle_{\rm full} = \sum_{N=-4}^{4} e^{iN\theta}\sum_y \langle \pi(x,y)\pi(0,0)\rangle^N_{\beta,m} R^N(\beta,m), \qquad (32)$$

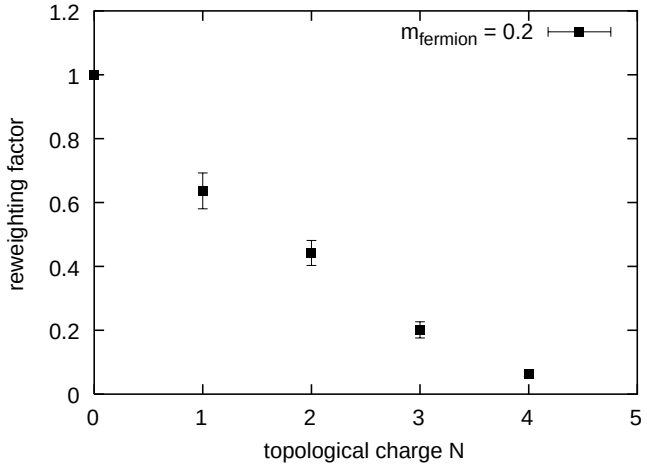

FIG. 5. The total reweighting factor $R^N(0.5,0.2)$ is plotted as a function of the topological charge. The factor falls off rapidly as the topological charge increases.

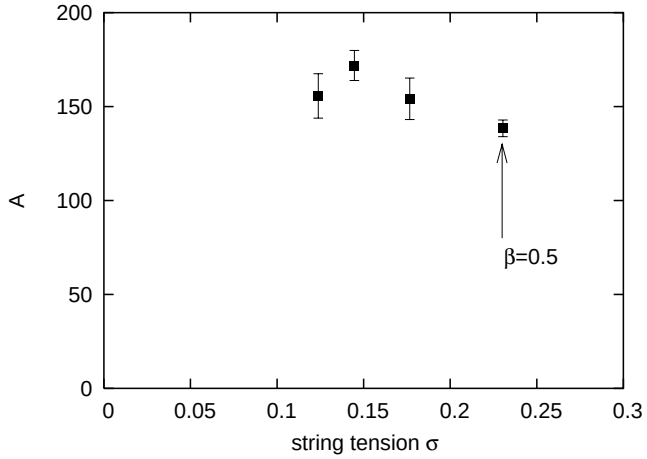

FIG. 6. Lattice spacing dependence of the dimensionless quantity $A\equiv m_\pi^6/(m^4\sigma)$. Horizontal axis is the string tension in lattice unit. The "string tension" is obtained from the logarithm of the expectation value of a plaquette in the $N=0$ sector.

up to a constant normalization factor. Here we have ignored $|N|>4$ sectors since they only give contributions less than 1.2% of zero sector for the pion. Then we can get the pion mass including full nonperturbative effects and θ dependence. In this calculation, the propagators are fitted by minimizing the χ^2 and the total statistical errors are estimated by summing those in individual sections in quadrature.

We compute the eta meson propagator in a similar manner as

$$\sum_y \langle \eta(x,y)\eta(0,0)\rangle_{\rm full} = \sum_{N=-4}^{4} e^{iN\theta}\sum_y \langle \eta(x,y)\eta(0,0)\rangle^N_{\beta,m} R^N(\beta,m). \qquad (33)$$

However, it seems that the propagator obtained by summing through $|N|\leqslant 4$ sectors does not saturate so that the truncation error is still large. Obviously, higher topological sectors are necessary. In this paper we only present the status of our exploratory studies but no definite quantitative results.

D. Systematic errors

In this section we discuss possible systematic errors. These error estimations show that our simulation is reasonable and the results are reliable.

Let us now study the lattice spacing dependence. We measure a dimensionless quantity $A\equiv m_\pi^6/(m^4\sigma)$ at $\beta=0.5,1.0,1.5,2.0$ in the zero topological sector, where m_π denotes pion mass and σ denotes the string tension defined from the logarithm of the plaquette expectation value in the zero sector. As Fig. 6 indicates, the results at $\beta=0.5$ show no large lattice spacing dependence which suggests that the discretization error is under control.

Next we discuss finite size effects for the space-time size L and for the extra dimension size L_3. We measure the pion

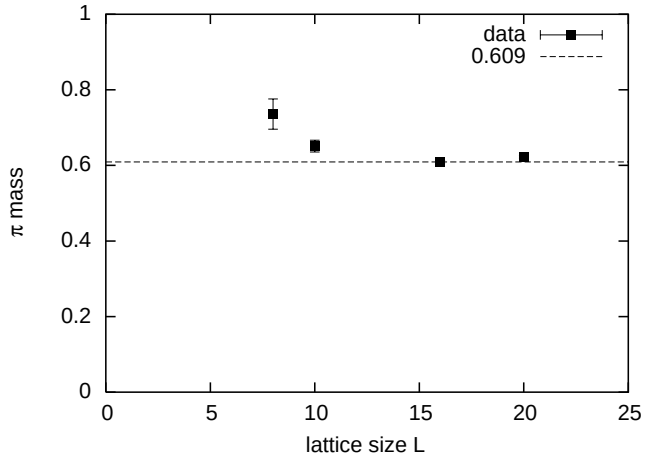

FIG. 7. The dependence of the pion mass on the lattice size L in the space-time direction measured in the zero sector. The fermion mass is $m=0.2$. Closed symbols are the data and the dashed line shows the fitted mass for $L=16$. The pion mass shows no volume dependence for $L \geqslant 16$.

mass on the lattices of size $L^2\times L_3=8^2\times 6$, $10^2\times 6$,$16^2\times 6$, $20^2\times 6$, $16^2\times 2$, $16^2\times 4$, and $16^2\times 10$ in the zero sector. Figure 7 shows L dependence and Fig. 8 shows L_3 dependence. We find that the meson mass is stable for L larger than 16 and for L_3 larger than 6 so that the finite size error is also under control with our choice of the lattice size $16^2\times 6$. The discretization error and finite size errors from the nonzero topological sector are similarly under control.

We now study the error in the integration over the moduli $\nu_{1,2}$. In order to estimate the systematic error we also evaluate the integral by the weighted sum of 10×10 points. We find that the change is very tiny (relative change $\sim 10^{-8}$) and is negligible compared to other systematic errors, as is expected from the mild ν dependence of $\det(D^0_{DW})^2/\det(D^0_{AP})^2$ in Fig. 3. Figure 3 also shows that $\det(D^N_{DW})^2/\det(D^N_{AP})^2$

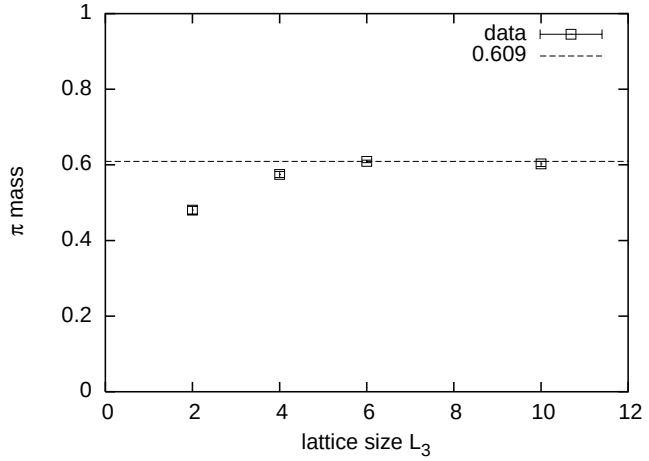

FIG. 8. The dependence of the pion mass on the lattice size L_3 in the third direction measured in the zero sector. The fermion mass is $m=0.2$. Open symbols are the data and the dashed line shows the fitted mass for $L_3=6$. The pion mass shows no volume dependence for $L_3 \geqslant 6$.

TABLE II. The reweighting factor in each sector from two different methods of evaluating the integral of $S^N_{\rm subtr}$; the trapezoidal rule and the integral of the polynomial fit. The resulting pion mass is are also given.

	By trapezoidal rule	By fit
$R^0(0.5,0.2)$	1.0	1.0
$R^1(0.5,0.2)$	0.637(56)	0.59(22)
$R^2(0.5,0.2)$	0.442(39)	0.45(16)
$R^3(0.5,0.2)$	0.201(25)	0.32(18)
$R^4(0.5,0.2)$	0.0636(91)	0.072(46)
m_π(at $\theta=0$)	0.647(7)	0.650(34)

with $N\neq 0$ has almost no ν dependence. In fact this remarkable flat dependence is also seen in the continuum counterpart analytically [39]. We therefore conclude that the error in the weighted sum is even more negligible for the nonzero topological sector.

Since the integral of $S^N_{\rm subtr}$ over β' is approximated by the trapezoidal rule using the data for the discrete set of β' points, the error in this approximation should be estimated. For this purpose we evaluate the integral of $S^N_{\rm subtr}$ in an alternative way, in which we fit the discrete set of data with the function of the form

$$S^N_{\rm subtr}(\beta',m)=\frac{a_1}{\beta'^2}+\frac{a_2}{\beta'^3}, \tag{34}$$

and compute the integral of $S^N_{\rm subtr}$ over β' analytically. Table II shows the difference of the two ways of evaluation. The pion masses are consistent with each other. Thus we find that the approximation for the integral of $S^N_{\rm subtr}$ does not give large systematic errors in the meson mass. We now study the truncation error in the sum over topological sectors. As we discussed before, we neglect $|N|>4$ sectors since these contributions are suppressed by a large value of action and fer-

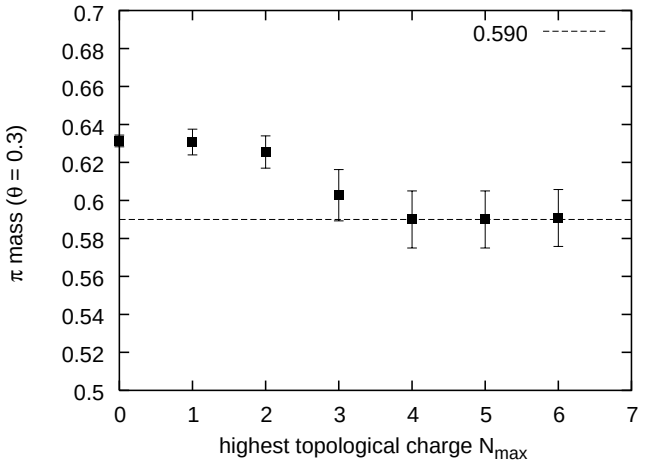

FIG. 9. The pion mass from the sum over $|N|\leqslant|N_{\rm max}|$ sector contributions for $m=0.2$ and $\theta=0.3\pi$. No change in the mass for $N_{\rm max}\geqslant 4$ is observed.

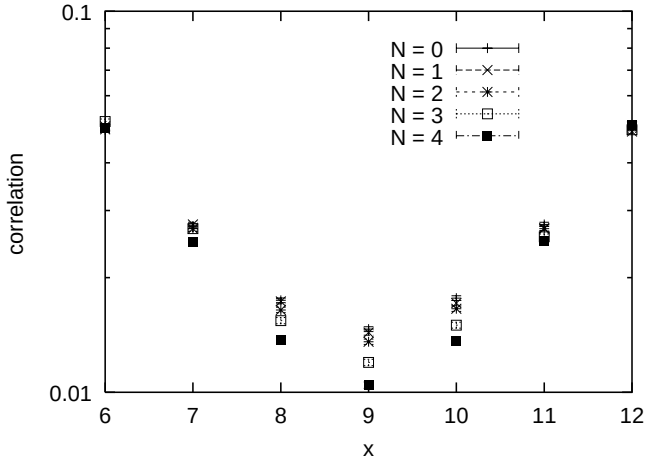

FIG. 10. The pion propagator in each sector for $m=0.2$.

mion zero modes. Figure 9 shows the pion mass at $\theta=0.3\pi$ measured for a variety of the highest topological charge $N_{\max}$. Therefore the truncation error in the sum over topological sectors are negligible in comparison with the statistical errors for the pion.

IV. MESON MASSES

A. Pion mass and θ dependence

Figure 10 shows pion propagators in each topological sector and Fig. 11 shows full propagators at various θ. We measure the pion mass by fitting these data to the hyperbolic cosine function. The fit range is $x=[5,8]$ for which we find a good plateau in the effective mass plot as shown in Fig. 12. In fitting χ^2/dof is also a small value ($\chi^2/dof<0.1$).

Figure 13 shows pion mass at $\theta=0$ as a function of fermion mass m. We ignore the m dependence of $S^N_{\rm subtr}(\beta',m)$ and use the $m=0.2$ result for all m. We fit the results to the following function suggested by the continuum theory with a possible additional constant term b from the residual mass of pion:

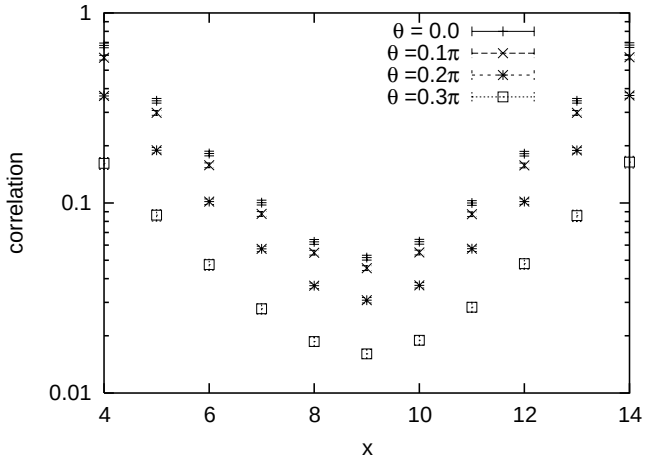

FIG. 11. The full pion propagators with $m=0.2$ for various θ are plotted.

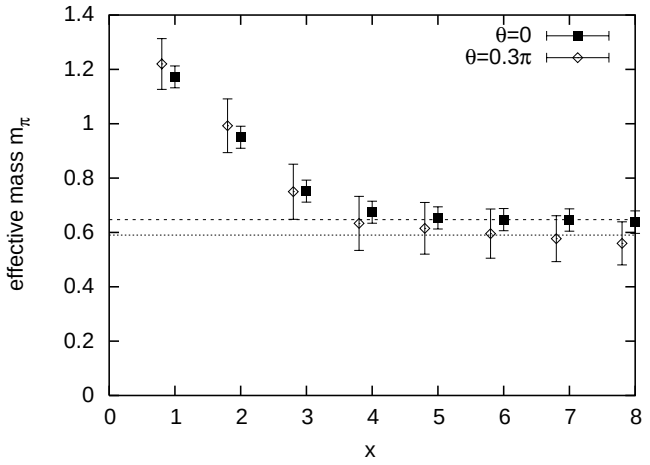

FIG. 12. The effective mass plot of the pion for $m=0.2$. Closed squares show the data for $\theta=0$ and the dashed line shows the result of the fit. Open diamonds show the data for $\theta=0.3\pi$ and the dotted line shows the fit result.

$$m_\pi(m)=am^{2/3}+b. \tag{35}$$

Figure 13 shows that Eq. (35) fits the data very well ($\chi^2/dof=0.39$) so that the fermion mass dependence is consistent with the continuum theory. The residual mass of the pion measured in the chiral limit is also tiny as $b=-0.057\pm0.060$, which shows that the violation of the chiral symmetry is very small.

In Fig. 14 we present the θ dependence of the pion mass at $\beta=0.5$ and $m=0.2$. As a remarkable feature, the result is in perfect agreement with that in the continuum theory in the $\theta/(2\pi)<0.5$ region. A good control of the θ dependence shows that our method for summing over different topological sectors with Lüscher's gauge action indeed works numerically.

At large θ statistical errors increase, due to cancellations of propagators among different topological sectors. In the

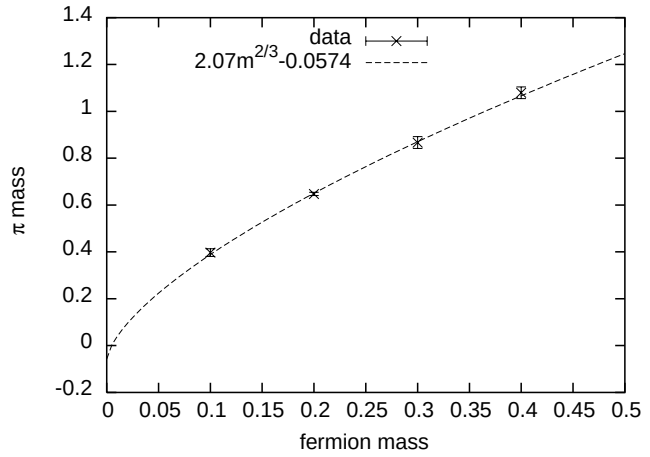

FIG. 13. The fermion mass dependence of the pion mass for $\theta=0$. The crosses are the lattice data and the dashed line is the result of the fit with the function in Eq. (35). The chiral behavior is consistent with that of continuum theory.

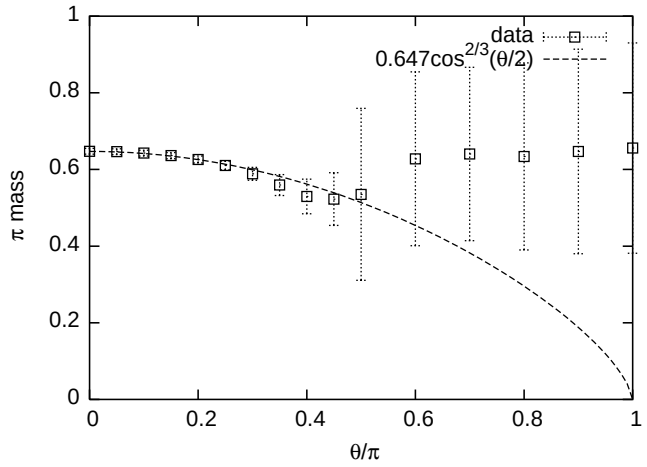

FIG. 14. θ dependence of the pion mass at $m=0.2$. The open symbols are the lattice data. The dashed line is the analytical result of the θ dependence in the continuum theory, where the normalization is fitted by the lattice results. For $\theta/(2\pi)<0.5$, the pion mass is proportional to $\cos(\theta/2)^{2/3}$, which is in complete agreement with the continuum results.

calculation, we approximate the integral of $S^N_{\rm subtr}(\beta',m)$ by the trapezoidal rule for the discrete set of β' points, but this does not seem to be the reason for the large fluctuation in the $\theta/(2\pi)>0.5$ region. The main nonperturbative contribution comes from Det^N and $S^N_{\rm subtr}(\beta',m)$ gives only perturbative effects of order β'^{-2}.

We suspect that this large fluctuation is an example of the well-known phase problem. Simply increasing the statistics might not improve the situation.

Of course in application to QCD, it will be important to evaluate $S^N_{\rm subtr}(\beta',m)$ and other observables more precisely.

B. η meson correlator and U(1) problem

As the final subject, we would like to present the result of our exploratory measurement of the η meson mass in order to study the topological structure. The η propagator consists of two parts:

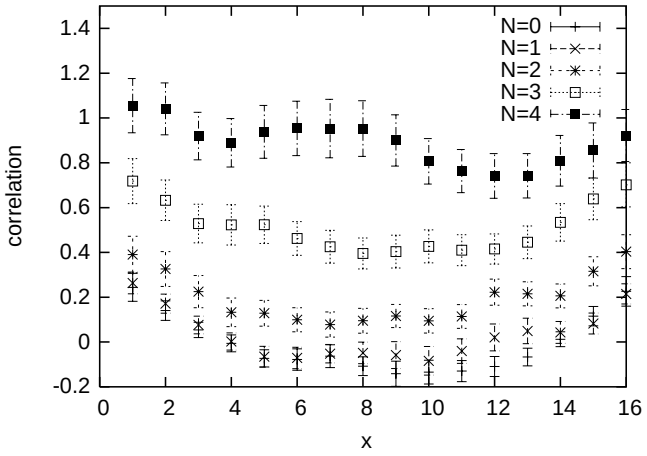

FIG. 15. The propagator of η in each sector at $m=0.2$.

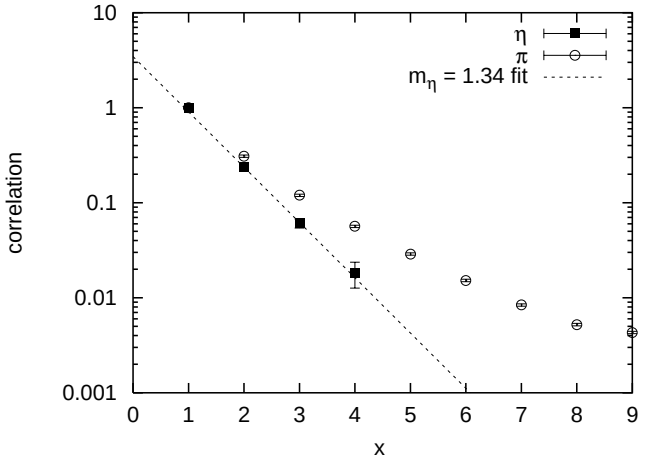

FIG. 16. The full propagator η at $m=0.2$ and $\theta=0$ (closed squares). The pion propagator is also plotted for comparison (open circles). The propagators are normalized by the value at $x=1$.

$$\langle \eta\eta\rangle = -2\left\langle \mathrm{tr}\left(\gamma_3 \frac{1}{D} \gamma_3 \frac{1}{D}\right)\right\rangle + 4\left\langle \mathrm{tr}\left(\gamma_3 \frac{1}{D}\right)\mathrm{tr}\left(\gamma_3 \frac{1}{D}\right)\right\rangle, \tag{36}$$

where the first term is the same as the flavor nonsinglet π propagator and the second term gives the ''hair-pin'' or disconnected contribution to the flavor singlet operator. Because the number of physical space-time points is only 16×16, we compute the ''hair-pin'' contribution by brute force, namely by solving the fermion propagator for all points without relying on the noise method [40] or Kuramashi method [41].

Figure 15 shows the contribution of the second term in each sector, whereas Fig. 16 shows the full (symmetrized) η propagator at $m=0.2$ and $\theta=0$. We also present effective mass plot in Fig. 17. We find that the fall of η propagator is steeper than that of π which gives qualitatively consistent results with the U(1) problem, although it suffers from both the theoretical errors as well as the large statistical errors making quantitative studies difficult. One of the major

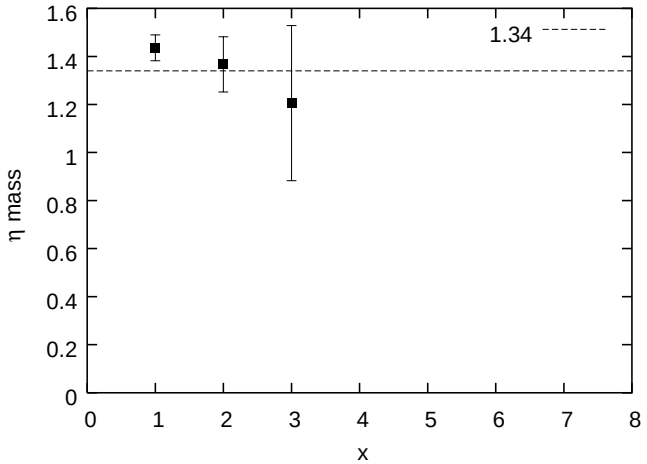

FIG. 17. The effective mass plot of the full η propagator for $m=0.2$, $\theta=0$. The dashed line shows the fit result.

sources of errors is the truncation in the topological sectors, since summation with topological charge for $N \leqslant 4$ does not show a satisfactory saturation unlike the case of the pion. Therefore further studies with a sufficiently larger number of topological sectors are necessary to confirm the stability of the data against the truncation. One also needs new ideas for efficiently reducing the statistical errors.

V. SUMMARY AND DISCUSSION

In this paper, we elucidate the role of the admissibility condition on the topological and chiral properties in lattice gauge theories by applying Lüscher's action together with domain wall fermions to a numerical simulation of the massive Schwinger model. To investigate the θ-dependence of the correlators, we have developed a method to sum over different topological sectors. We have found that Lüscher's action is indeed applicable to Monte Carlo simulations and all the results are consistent with those in the continuum theory, confirming the validity of our method.

We summarize the features of this action here again. (1) In Lüscher's action, the gauge field strength is uniquely determined from the plaquette and the gauge action is a smooth function of the field strength. (2) The range of the action is not compact;

$$0 \leqslant S_G < \infty. \tag{37}$$

This is the same situation as continuum theory. We can treat the theory in terms of the field strength rather than plaquettes. According to these features, Lüscher's gauge action has many advantages.

(1) The use of this gauge action with the domain wall fermion action is valid even for the strong coupling regime since unphysical configurations are suppressed. (We find the suppression effect is especially remarkable in quenched approximation as discussed in the Appendix.)
(2) We can treat the topological properties of the lattice theories precisely. This exact topological treatment is useful not only mathematically but also in a practical point of view. In the conventional approach, there are two technical problems, i.e., violation of chirality at strong coupling and the slowing down of the topology change in unquenched simulation. For the former problem, the improved gauge actions which suppress the dislocations are proposed. However, in principle the suppression of the dislocations also suppresses the topology change so that the latter problem becomes even more difficult. Our method makes the improvement to the extreme and prohibits both the dislocation and the topology change completely, however, by computing each topological sector and its reweighting factor we can reconcile the solutions to the topology change problem and the dislocation problem at the same time.
(3) Once each topological sector can be computed separately, we can obtain a θ dependence at once.
(4) Aside from the fact that we must simulate for each sector the typical simulation, time needed for the trivial topological sector is no larger than that of using Wilson's plaquette action. For the nonzero topological charge sector, one can also increase the statistics at will very efficiently, in contrast to the conventional method where one can increase the statistics only by reaching the thermal equilibrium. In this sense, our method would have advantages in physical quantities for which the topological sectors with larger instanton numbers give larger contributions.

It will be interesting to explore the possibility of applying Lüscher's type of gauge action to QCD in four dimensions. The reweighting factor, however, would not be easy to calculate since the Dirac matrix is very large and the exact topological index as well as the structure of the gauge field space are much more complicated in four-dimensional torus [9]. Moreover, one should find the minimum of the gauge action in each sector since the self-dual classical solutions are not known in some cases. We still hope that the under-

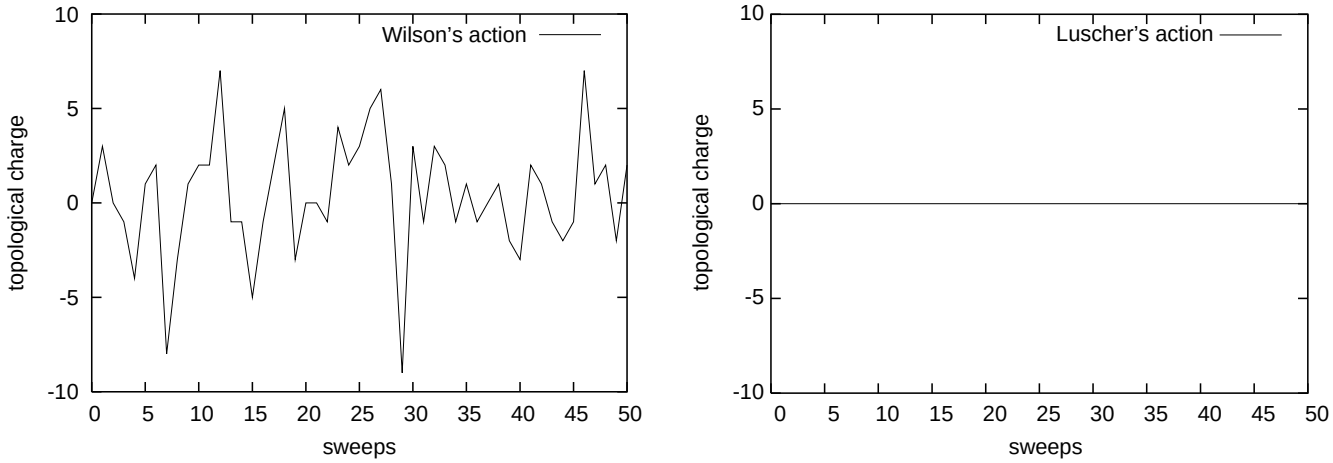

FIG. 18. The Monte Carlo evolutions of the topological charge in the quenched calculation with Wilson's gauge action and Lüscher's gauge action for the gauge couplings having the same string tension. Left: Wilson's gauge action at $\beta = 3.4$. Right: Lüscher's gauge action at $\beta = 1.0$. Lüscher's gauge action shows no topology change.

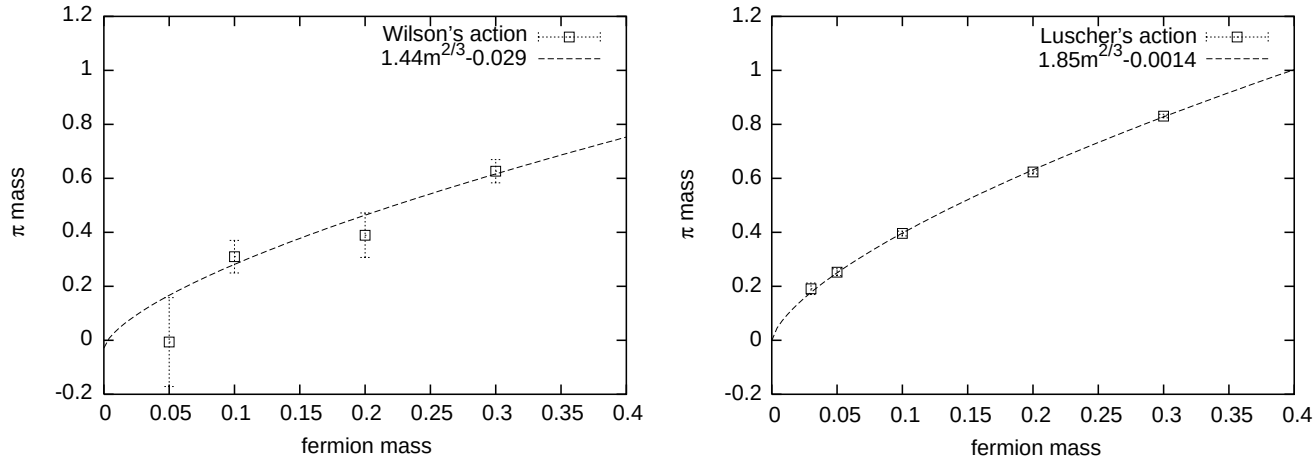

FIG. 19. The chiral behaviors of the pion mass in the quenched calculation with Wilson's gauge action and Lüscher's gauge action for the gauge couplings having the same string tension. In this quenched study, 100 configurations with $N=0$ are taken for the calculation with each action. Left: Wilson's gauge action at $\beta=3.4$. Right: Lüscher's gauge action at $\beta=1.0$. Wilson's gauge action suffers from large fluctuation while Lüscher's gauge action shows a good chiral behavior. Both of them are calculated by domain-wall fermions.

standing of the topological properties in lattice QCD will be improved by applying Lüscher's admissibility condition.

ACKNOWLEDGMENTS

We acknowledge Hideo Matsufuru and Ayumu Sugita for discussions and help throughout all stages of this work and Hideo Matsufuru also for his careful reading of the manuscript and his comments. We would also like to thank Yoshio Kikukawa for his beautiful lectures as well as private discussions on recent developments in chiral gauge theories on the lattice. We are also grateful to Kenichi Shizuya, Masanori Okawa, Yusuke Taniguchi, Yoshinobu Kuramashi, and Yasumichi Aoki for useful discussions. The authors thank the Yukawa Institute for Theoretical Physics at Kyoto University, where this work was initiated during the YITP-W-02-15 on ''YITP School on Lattice Field Theory.'' The numerical simulations were done on the Alpha workstation at Yukawa Institute for Theoretical Physics in Kyoto University, NEC SX-5 at Research Center for Nuclear Physics in Osaka University, and Hitachi SR8000 model F1 supercomputer at KEK.

APPENDIX

In this appendix, we examine the validity of Lüscher's action in the quenched approximation. We set the lattice size to be $32\times32\times5$ and measure the pion mass. Gauge coupling β is chosen to give the same string tension $\sigma=0.18$; $\beta=1.0$ for Lüscher's action and $\beta=3.4$ for Wilson's action.

Figure 18 shows the evolution of the topological charge. Since the zero modes in the fermion determinants are all neglected in the quenched approximation with Wilson action, there is no suppression on topology changes. On the other hand, Lüscher's action never allows topology changes. Moreover, one can see that the fermion mass dependence of the pion mass is much better with Lüscher's action than that of $N=0$ configurations with Wilson's action as is clear in Fig. 19. In fact, by fitting the results to the function am^b we obtain

$$b=0.768\pm0.194 \quad \text{(Wilson)},$$

$$b=0.649\pm0.025 \quad \text{(Lüscher)}. \tag{A1}$$

The index b with Lüscher's action is very close to 2/3.

For a theoretically complete study of the quenched Schwinger model, we should take a sum over different topological sectors and compare with analytic result in which it is predicted that the quenching effect does give a different fermion mass dependence from that in the unquenched theory [27].

[1] H.B. Nielsen and M. Ninomiya, Phys. Lett. **105B**, 219 (1981).
[2] H.B. Nielsen and M. Ninomiya, Nucl. Phys. **B185**, 20 (1981); **B195**, 541(E) (1982).
[3] H.B. Nielsen and M. Ninomiya, Nucl. Phys. **B193**, 173 (1981).
[4] P.H. Ginsparg and K.G. Wilson, Phys. Rev. D **25**, 2649 (1982).
[5] H. Neuberger, Phys. Lett. B **417**, 141 (1998).
[6] H. Neuberger, Phys. Lett. B **427**, 353 (1998).
[7] M. Lüscher, Phys. Lett. B **428**, 342 (1998).
[8] M. Lüscher, Nucl. Phys. **B549**, 295 (1999).
[9] M. Lüscher, Commun. Math. Phys. **85**, 39 (1982).
[10] M. Lüscher, Nucl. Phys. **B538**, 515 (1999).
[11] Y. Iwasaki, UTHEP-118 (1983).
[12] M.G. Alford, W. Dimm, G.P. Lepage, G. Hockney, and P.B. Mackenzie, Phys. Lett. B **361**, 87 (1995).

[13] T. Takaishi, Phys. Rev. D **54**, 1050 (1996).
[14] QCD-TARO Collaboration, P. de Forcrand *et al.*, Nucl. Phys. **B577**, 263 (2000).
[15] CP-PACS Collaboration, A. Ali Khan *et al.*, Phys. Rev. D **63**, 034502 (2001).
[16] L.I. Wu (RIKNE-BNL-CU), Nucl. Phys. B (Proc. Suppl.) **83**, 224 (2000); Y. Aoki *et al.*, hep-lat/0211023.
[17] C. Jung, R.G. Edwards, X.D. Ji, and V. Gadiyak, Phys. Rev. D **63**, 054509 (2001).
[18] M. Lüscher, Nucl. Phys. **B568**, 162 (2000).
[19] A. Jaster, hep-lat/9605011.
[20] D.B. Kaplan, Phys. Lett. B **288**, 342 (1992).
[21] Y. Shamir, Nucl. Phys. **B406**, 90 (1993); V. Furman and Y. Shamir, *ibid.* **B439**, 54 (1995).
[22] C.R. Gattringer, I. Hip, and C.B. Lang, Nucl. Phys. **B508**, 329 (1997).
[23] C.R. Gattringer, I. Hip, and C.B. Lang, Phys. Lett. B **409**, 371 (1997).
[24] C. Gattringer, I. Hip, and C.B. Lang, Phys. Lett. B **466**, 287 (1999).
[25] H. Dilger and H. Joos, Nucl. Phys. B (Proc. Suppl.) **34**, 195 (1994).
[26] F. Farchioni, I. Hip, and C.B. Lang, Phys. Lett. B **443**, 214 (1998).
[27] S. Dürr and S.R. Sharpe, Phys. Rev. D **62**, 034506 (2000).
[28] S. Dürr, Phys. Rev. D **62**, 054502 (2000).
[29] S. Elser, Ph.D. thesis, Humboldt University, 2001, hep-lat/0103035.
[30] P. de Forcrand, J.E. Hetrick, T. Takaishi, and A.J. van der Sijs, Nucl. Phys. B (Proc. Suppl.) **63**, 679 (1998).
[31] P.M. Vranas, Phys. Rev. D **57**, 1415 (1998).
[32] S. Elser and B. Bunk, Nucl. Phys. B (Proc. Suppl.) **53**, 953 (1997).
[33] J.S. Schwinger, Phys. Rev. **128**, 2425 (1962).
[34] S.R. Coleman, R. Jackiw, and L. Susskind, Ann. Phys. (N.Y.) **93**, 267 (1975).
[35] S.R. Coleman, Ann. Phys. (N.Y.) **101**, 239 (1976).
[36] J. Frohlich and E. Seiler, Helv. Phys. Acta **49**, 889 (1976).
[37] S. Dürr, Nucl. Phys. B (Proc. Suppl.) **106**, 598 (2002).
[38] *Numerical Recipes in* FORTRAN, 2nd ed., edited by W.H. Press, S.A. Teukolsky, W.T. Vetterling, and B.P. Flannery (Cambridge University Press, Cambridge, England, 1992).
[39] S. Azakov, Fortschr. Phys. **45**, 589 (1997).
[40] K. Bitar *et al.*, Nucl. Phys. **B313**, 348 (1989); H.R. Fiebig and R.M. Woloshyn, Phys. Rev. D **42**, 3520 (1990).
[41] Y. Kuramashi *et al.*, Phys. Rev. Lett. **72**, 3448 (1994); M. Fukugita *et al.*, Phys. Rev. D **51**, 3952 (1995).